

A Computational Study on Radiation Shielding Potentials of Eutectic High Entropy Alloys

Zeynep AYGUN^{*1}, Murat AYGUN²

^{*1}Bitlis Eren University, Vocational School of Technical Sciences, 13100, Bitlis, Türkiye
zeynep.yarbasi@gmail.com (ORCID: 0000-0002-2979-0283)

²Bitlis Eren University, Faculty of Science and Arts, Department of Physics, 13100, Bitlis, Türkiye
mavgun@beu.edu.tr (ORCID: 0000-0002-4276-3511)

Abstract

Eutectic high entropy alloy, a new kind of high entropy alloy, has great interest due to the widespread use in high temperature applications with perfect mechanical features. Our motivation to do this work is the absence of studies about the radiation shielding performances of this new type alloys. The aim of the work was to determine the photon protection parameters such as linear and mass attenuation coefficients, mean free path, half value layer, effective atomic number, fast neutron removal cross section and buildup factors of the eutectic high entropy alloys, (CoCrFeNiNb_{0.25}Ta_{0.20}; CoCrFeNiTa_{0.4}; CoCrFeNiTa_{0.75}; CoCrFeNiTa_{0.25}Hf_{0.25}; Co₂MoxNi₂VW_x) by using Phy-X/PSD software. XCom was also performed to obtain the mass attenuation coefficients of the alloys, and a good agreement was obtained. It was concluded that Co₂MoxNi₂VW_x has the most shielding property while CoCrFeNiNb_{0.25}Ta_{0.20} shows the least shielding feature among the alloys. It was also determined that Co₂MoxNi₂VW_x has the highest neutron shielding ability. As a result, it is noted that eutectic high entropy alloys can be evaluated as new type shielding materials for radiation related applications.

Keywords: Photon protection parameters, EHEAs, Phy-X/PSD.

Received: 15.05.2023

Accepted: 29.06.2023

Published: 30.06.2023

*Corresponding author: Zeynep AYGÜN, Bitlis Eren University, Vocational School of Technical Sciences, 13100, Bitlis, Türkiye.

E-mail: zeynep.yarbasi@gmail.com

Cite this article as: Z. Aygün and M. Aygün., A Computational Study on Radiation Shielding Potentials of Eutectic High Entropy Alloys, Eastern Anatolian Journal of Science, Vol. 9, Issue 1, 7-15, 2023.

1. Introduction

Since reported firstly by Cantor et al. (2004) and Yeh et al. (2004), high entropy alloys (HEAs) are the new alloy systems consisting of at least four major elements. HEAs with perfect mechanical, thermal and chemical properties have great interest from researchers (Aygün 2023; Sakar et al. 2023; Chen et al. 2023; Xiao et al. 2020). Recently, eutectic HEAs (EHEAs) have been proposed as a kind of HEAs firstly by Lu et al. (2014) by adding an appropriate element to the HEA. The combination of FCC (ductile phase) with BCC or intermetallic ones (hard phase) with good creep resistance and stable defect structures makes the alloys attractive for the studies in high temperature applications. The microstructure features of the EHEAs are also effective for radiation resistance in materials (Wang et al. 2023). EHEAs can be used in several industries, such as aerospace, automotive, electronics, etc. Therefore, recently, many researches have been carried out by developing eutectic microstructures for the purpose of obtaining better combination of mechanical properties (Wang et al. 2023; Jiao et al. 2023; Mukarram et al. 2021; Li et al. 2022; Chen et al. 2021).

Increasing application areas of radiation and technological developments necessitate the production of effective radiation shielding materials for human health. The alloys used in high temperature and radiation related applications were studied for their radiation shielding performances previously (Xiao et al. 2020; Chen et al. 2023; Sakar et al. 2023; Aygün, 2023; Aygün and Aygün, 2023). But, the new type EHEAs have not been studied by radiation protection features, yet. The objective of determining radiation shielding properties of the EHEAs is necessary for closing this lack in the literature. The linear and mass attenuation coefficients (LAC and MAC), effective atomic number (Z_{eff}), mean free path

(MFP), half value layer (HVL), atomic cross section (ACS), electronic cross section (ECS), fast neutron removal cross section (FNRCs) and build up factors (EBF and EABF) are the photon protection parameters which are significant to learn the degree of protection of the alloys. In this regard, for the purpose of estimating the photon protection performances of the alloys (CoCrFeNiNb0.25Ta0.20/D1; CoCrFeNiTa0.4/D2; CoCrFeNiTa0.75/D3; CoCrFeNiTa0.25Hf0.25/D4; Co2MoxNi2VWx/D5) Phy-X/PSD developed for shielding, photon attenuation and dosimetry including a wide energy range of 1 keV-100 GeV was used. XCom software (Berger and Hubbell, 1987) was also used which is developed to acquire photon interaction cross-sections and MAC values of an element, compound or mixture in the 1 keV–100 GeV wide energy region.

2. Materials and Methods

In the study, EHEAs reported previously for their mechanical properties were chosen. The chemical components of the alloys were used for the calculations (Jiang et al. 2016; Jiang et al. 2018; Mukarram et al. 2021; Jiao et al. 2023) and given in Table 1.

The rule of mixture is used for calculation of density (ρ_{mix}) of the alloys (Xiang et al. 2019):

$$\rho_{mix} = \frac{\sum_{i=1}^n c_i A_i}{\sum_{i=1}^n c_i A_i / \rho_i} \quad (1)$$

A_i , c_i and ρ_i , and are atomic fraction, atomic weight of element i_{th} and density, respectively.

The MAC can be found by the Eq. 2:

$$I = I_0 e^{-\mu t} \quad (2)$$

$$\mu_m = \frac{\mu}{\rho} = \ln(I_0/I) / \rho t = \ln(I_0/I) / t_m \quad (3)$$

where μ (cm^{-1}) is the linear and μ_m (cm^2/g) is the mass attenuation coefficients, respectively.

MAC can be also determined by Eq. 4 (Jackson and Hawkes, 1981);

$$\mu/\rho = \sum_i w_i (\mu/\rho)_i \quad (4)$$

w_i is the weight fraction and $(\mu/\rho)_i$ is the MAC of the i_{th} constituent element.

ACS (σ_a) can be obtained by the equation formulated as;

$$ACS = \sigma_a = \frac{N}{N_A} (\mu/\rho) \quad (5)$$

N_A is the Avogadro's number and N is the atomic mass of materials.

ECS (σ_e) is found by the equation (Han & Demir 2009a);

$$ECS = \sigma_e = \frac{\sigma_a}{Z_{eff}} \quad (6)$$

Z_{eff} can be found by Eq. 7 (Manohara and Hanagodimath, 2007).

$$Z_{eff} = \sigma_a / \sigma_e \quad (7)$$

HVL and MFP are calculated by Eqs. 8-9;

$$HVL = \frac{\ln(2)}{\mu} \quad (8)$$

$$MFP = \frac{1}{\mu} \quad (9)$$

EBF and EABF can be obtained by the equations below (Harima et al. 1986; Harima, 1993). Geometric progression (G-P) fitting parameters for the alloy are determined by in Eq. 11 (ANSI/ANS, 1991). Buildup factors can be determined by Eq. 12 and 13, determining $K(E, x)$ in Eq. 14.

$$Z_{eq} = \frac{Z_1(\log R_2 - \log R) + Z_2(\log R - \log R_1)}{\log R_2 - \log R_1} \quad (10)$$

$$F = \frac{F_1(\log Z_2 - \log Z_{eq}) + F_2(\log Z_{eq} - \log Z_1)}{\log Z_2 - \log Z_1} \quad (11)$$

$$B(E, x) = 1 + \frac{(b-1)(K^x - 1)}{(K-1)} \quad \text{for } K \neq 1 \quad (12)$$

$$B(E, x) = 1 + (b-1)x \quad \text{for } K=1 \quad (13)$$

$$K(E, x) = cx^a + d \frac{\tanh\left(\frac{x}{X_k} - 2\right) - \tanh(-2)}{1 - \tanh(-2)} \quad \text{for } x \leq 40 \text{ mfp} \quad (14)$$

The R_1 and R_2 values are the $(\mu_m)_{\text{Compton}}/(\mu_m)_{\text{Total}}$ the adjacent elements with Z_1 and Z_2 atomic numbers. F is the (G-P) fitting parameters (a , b , c , d , X_k coefficients) of the sample. F_1 and F_2 are the G-P fitting parameters for Z_1 and Z_2 atomic numbers at an energy, respectively. X and E are penetration depth and primary photon energy, respectively.

The FNRCs (\sum_R) value of the material is determined as follows (Sakar, 2020; Woods, 2013):

$$\sum_R = \sum_i \rho_i (\sum_R / \rho)_i \quad (15)$$

where ρ_i is the partial density of the compound and $(\sum_R / \rho)_i$ is the mass RCS of the i_{th} constituent element.

3. Results

Based on the chemical components of EHEAs were taken from literature (Table 1) and the photon-matter interaction parameters of the alloys were determined. Dependences of the found MAC values versus photon energies (1keV-100GeV) are given in Fig. 1(a). At low (1-100keV), mid (100keV-5MeV) and high (>5 MeV) energies MAC values decreased apparently with increasing energy, a little changed and increased with increasing energy under the effect of the photoelectric (PE), Compton scattering (CS) and pair production (PP), respectively. XCom was also used to calculate the MAC values of the EHEAs to see the agreement of the results by Phy-X/PSD (Fig. 1). The MAC values of the RHE alloys and formerly studied super alloys for several energies are given in Table 2.

Table 1. Chemical compositions of the studied EHEAs.

Sample/S ample code	CoCrFeNi Nb0.25Ta /D1	CoCrFe NiTa0.4 /D2	CoCrFe NiTa0.7 5/D3	CoCrFeNi Ta0.25Hf0 .25/D4	Co2Mo xNi2V Wx/D5
Co	22.28	22.81	21.1	21.80	25.74
Fe	22.53	21.45	21.1	22.03	-
Nb	4.900	-	-	-	-
Ta	4.500	12.64	15.6	5.480	-
Ni	22.56	21.44	21.1	22.07	19.62
Cr	23.23	21.66	21.1	22.77	-
Hf	-	-	-	5.860	-
W	-	-	-	-	23.60
V	-	-	-	-	10.19
Mo	-	-	-	-	20.85
Density	8.709	9.572	9.897	9.258	13.155

Variation of the calculated LAC values as a function of photon energies (1keV-100GeV) is given in Fig. 1(c). LAC is the parameter used for obtaining MAC, HVL and MFP parameters. Due to the density effect, bigger differences are observed for LAC values. D5 alloy has the biggest LAC value while D1 alloy has the lowest one at the same energy.

The HVL and MFP are the other parameters related to thickness. HVL and MFP values varying as a function of energies calculated by the code are seen in Fig. 2. At the energies dominant by CS, most photons have a high probability of scattering. So, thicker materials are required because their absorption probability is lower and the MFP of photons is longer. Having lower values of HVL and MFP at high energies indicates better shielding capability. The HVL values in the same energy region are ordered as D5<D3<D2<D4<D1. The ascending order of MFP

values is D5<D3<D2<D4<D1. Based on the found results, alloy D5 has the lowest HVL and MFP values, whereas D1 alloy has the highest ones. Therefore, it can be noted that D5 has the highest shielding feature among the alloys. The shielding capacity of the EHEAs are analyzed by the comparison of HVL values with those of previously given alloys and shown in Fig. 2(b).

The probability of interaction per electron and per atom per unit volume of a material is named as ECS and ACS, respectively. Varying of ECS and ACS results as a function of photon energies are seen in Fig. 3. If the alloy has greater values of ACS and ECS, it can be considered as a better protective alloy. Based on the values of ACS and ECS, the shielding potential of the D5 alloy is the highest among them.

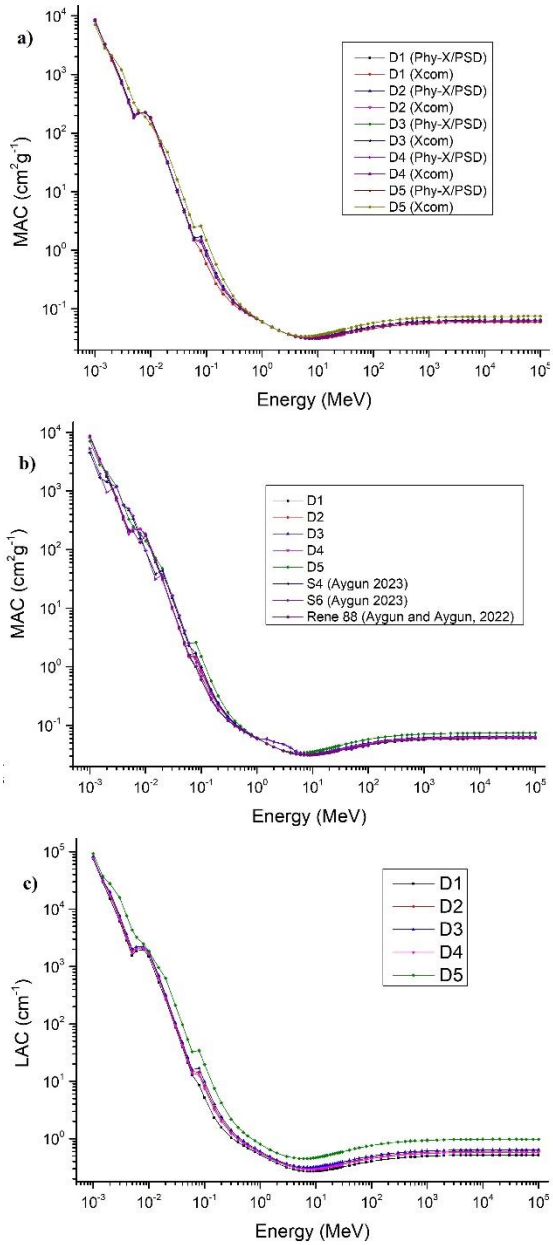


Figure 1. The variations of MAC (a) MAC of other alloys (b) and LAC (c) values versus photon energies.

Z_{eff} values varying versus photon energies are seen in Fig. 4. PE effect causes maximum Z_{eff} values at low energies. The highest Z_{eff} at ≈ 0.005 MeV can be observed by the K-absorption edge of Cr and that at ≈ 0.07 MeV can be observed for K-absorption edge of Ta and W as seen in Fig. 4. The values decreased apparently, then increased with increasing energy and stayed constant in the higher energies. The highest Z_{eff} values are achieved for D5 with the presence of W and Mo (higher atomic numbers); whereas lowest

Z_{eff} values are observed for D1 with no contribution of Hf, Mo and W. Thus, D5 alloy shows the highest shielding potential, while D1 shows the lowest shielding property.

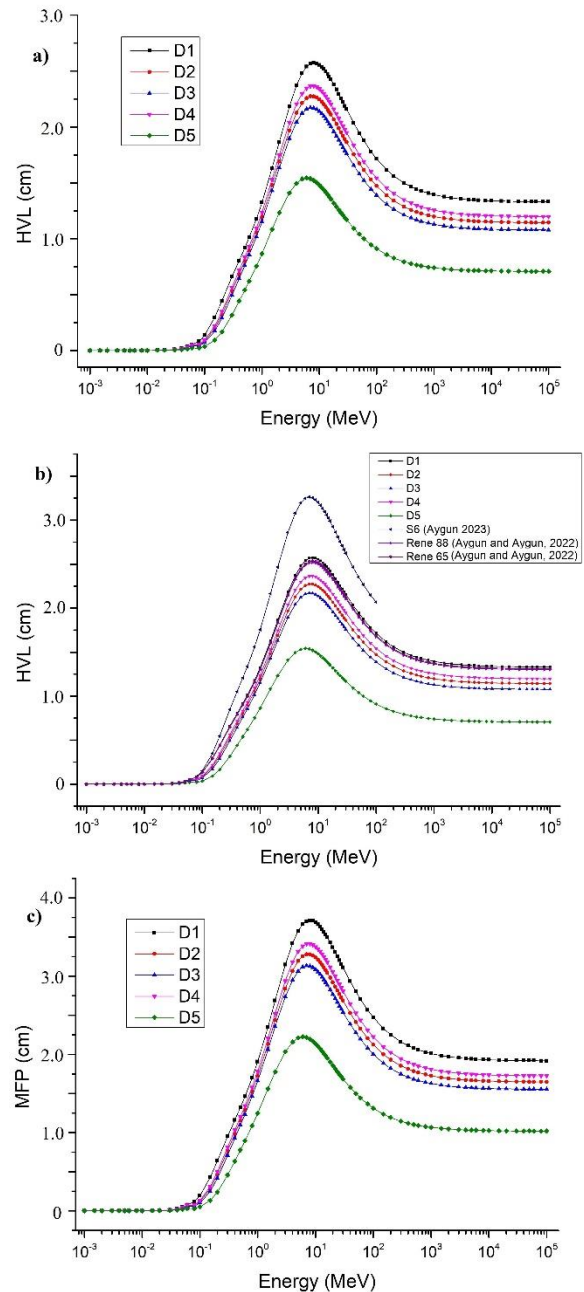


Figure 2. The variations of HVL (a) HVL of other alloys (b) and MFP (c) values versus photon energies.

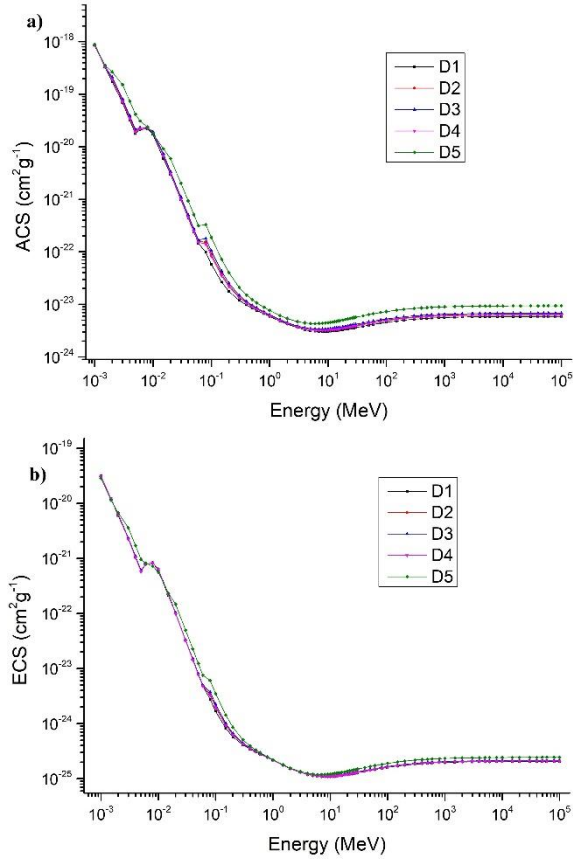


Figure 3. The variations of ACS (a) and ECS (b) values versus incident energy.

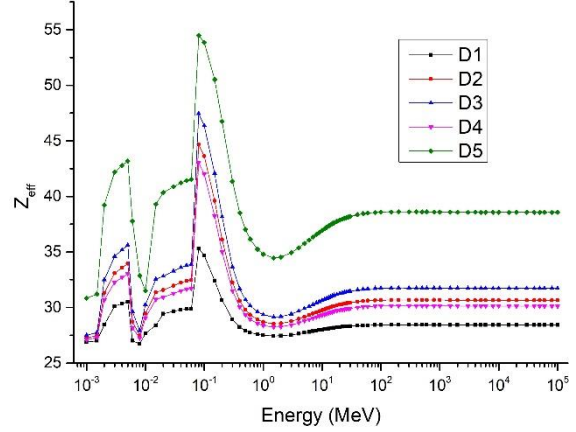


Figure 4. The variations of Z_{eff} values versus incident energy.

Table 2. Comparison of the MAC values for the EHEAs and previously reported alloys.

Energy (MeV)	D1	D2	D3	D4	D5	Rene 80 (Aygun and Aygun, 2022)	Rene 95 (Aygun and Aygun, 2022)	Inc 617 (Aygun and Aygun, 2023)	Inc 800HT (Aygun and Aygun, 2023)	In625 (Sayed et al. 2020)	In718 (Sayed et al. 2020)
0.015	60.61	68.41	70.62	67.03	72.63	64.38	63.06	59.14	60.60	65.70	59.00
0.03	9.957	10.17	10.56	9.931	16.12	10.44	10.83	10.83	8.763	9.549	10.41
0.05	2.420	2.498	2.607	2.432	4.047	2.537	2.633	2.626	2.101	2.287	2.51
0.8	0.068	0.069	0.069	0.068	0.070	0.068	0.068	0.068	0.067	0.068	0.067
1	0.060	0.061	0.061	0.061	0.061	0.061	0.061	0.060	0.060	0.061	0.060
3	0.036	0.037	0.037	0.037	0.037	0.037	0.037	0.037	0.036	0.037	0.037
5	0.032	0.033	0.033	0.033	0.034	0.033	0.033	0.032	0.032	0.032	0.032
8	0.031	0.032	0.032	0.032	0.036	0.031	0.032	0.031	0.030	0.031	0.031
10	0.031	0.032	0.033	0.032	0.036	0.032	0.032	0.031	0.030	0.031	0.031
100	0.046	0.049	0.050	0.049	0.058	0.047	0.047	0.046	0.044	-	-
1000	0.057	0.060	0.062	0.060	0.071	0.058	0.058	0.057	0.054	-	-

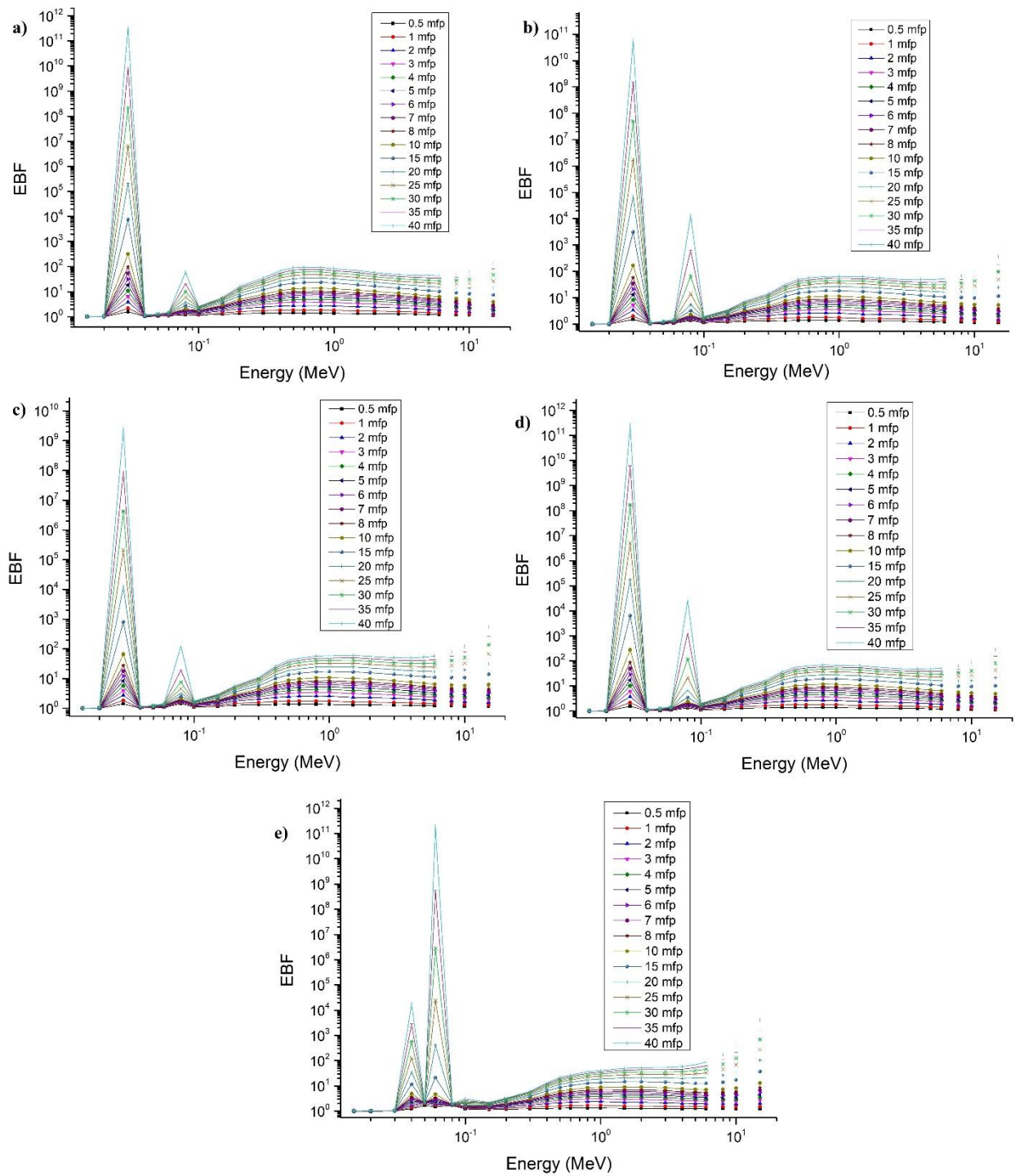


Figure 5. The variations of EBF values of D1 (a) D2 (b) D3 (c) D4 (d) D5 (e) versus photon energies.

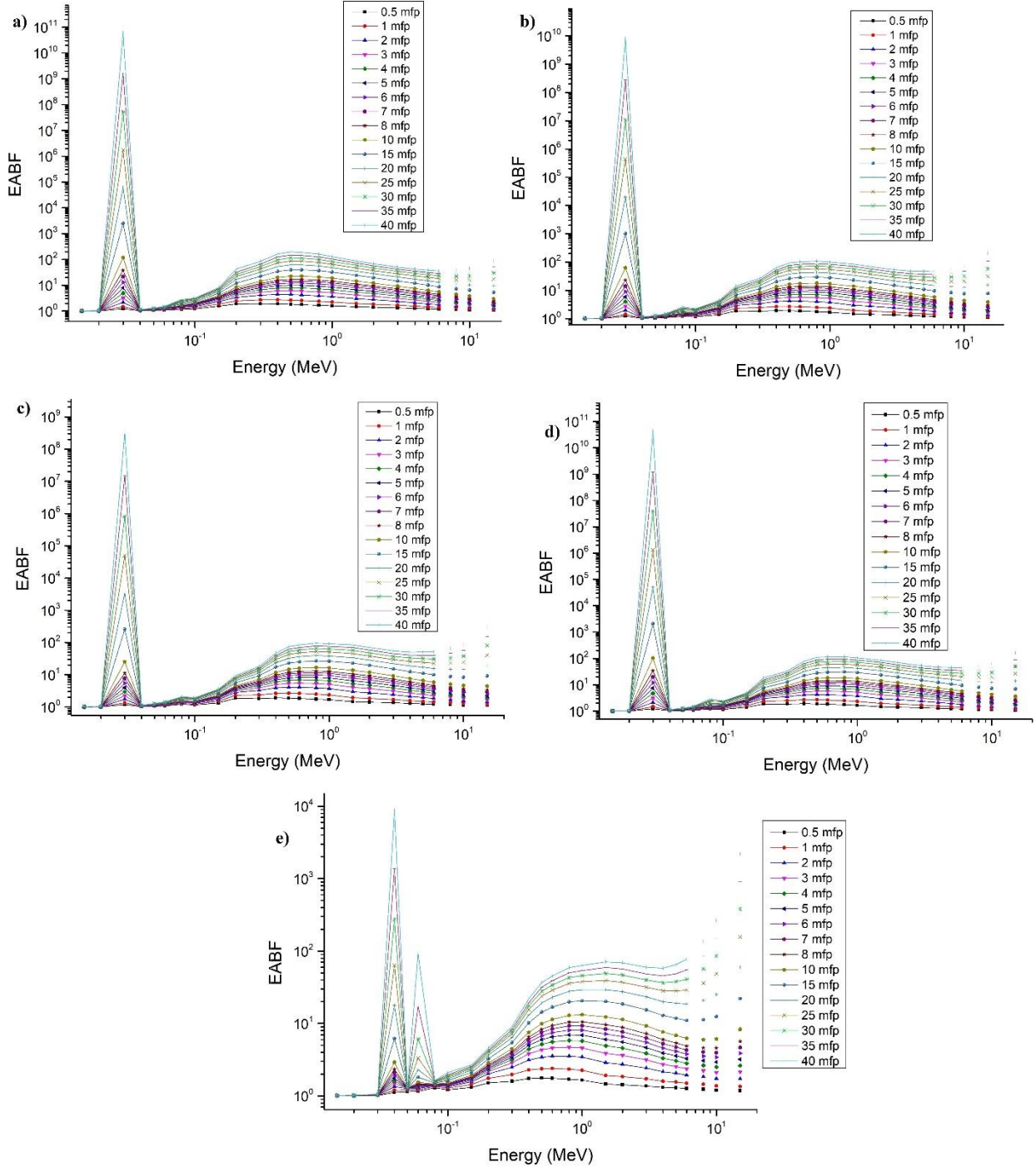


Figure 6. The variations of EABF values of D1 (a) D2 (b) D3 (c) D4 (d) D5 (e) versus photon energies.

EABF and EBF of the EHEAs were obtained for 16 penetration depths by Phy-X/PSD. The changes of buildup factors versus photon energies are given in Figs. 5-6. In PE region, buildup factors are small due to the fact that photons with low-energies are absorbed by their all energies. In CS region, since the large number of photons are scattered, photon

accumulation increased and the factors achieve highest values in the mid-energy region. In PP region, photons are absorbed strongly. Hereby, the buildup factors have lower values at high energies. Depending on the values of EABF and EBF, the lowest photon cluster is observed for D5 EHEA than the other

alloys. The peak observed at ≈ 0.07 MeV can be due to K-absorption edge of Ta or W (Aygün, 2023).

FNRCs values of the EHEAs were determined and given in Fig. 7. It can be said that the highest value is obtained for D5 and the lowest one is for D1.

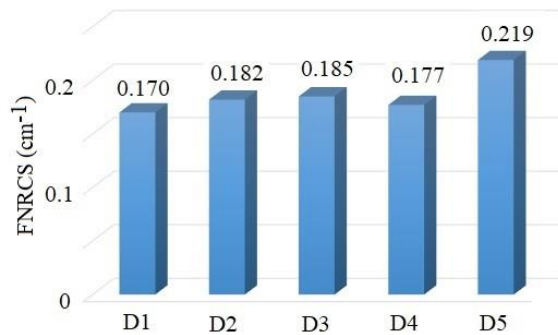


Figure 7. FNRCs values of the EHEAs.

4. Conclusions

In the paper, photon protection parameters of EHEAs were calculated by Phy-X/PSD code in the energies of 1 keV-100 GeV to learn the photon protection abilities. Xcom was also used for obtaining MAC values and it is seen that the results are compatible. It was examined that HVL values of the EHEAs are lower than those of previously reported alloys. It can be also mentioned that Co₂MoxNi₂VWx has highest shielding ability than the others, while CoCrFeNiNb_{0.25}Ta_{0.20} has the lowest shielding property among the alloys. In general, the shielding performances of the alloys can be ordered as D5>D3>D2>D4>D1. Obtained FNRCs values make possible to use the alloys also for neutron shielding. Consequently, it is north worthy to say that the EHEAs can be estimated as new kind of shielding materials in radiation related areas with their superior features.

References

- AYGÜN, Z. (2023) Study on Radiation Shielding Characteristics of Refractory High Entropy Alloys by EpiXS Code. *Acta Physica Polonica A* 1(143):66-74.
- AYGÜN, Z., AYGÜN, M., (2023). Evaluation of radiation shielding potentials of Ni-based alloys, Inconel-617 and Incoloy-800HT,

candidates for high temperature applications especially for nuclear reactors, by EpiXS and Phy-X/PSD codes, *J. Polytech.* in press (2023).

<https://doi.org/10.2339/politeknik.1004657>

- AYGÜN, Z., AYGÜN, M., (2022). Radiation Shielding Potentials of Rene Alloys by Phy-X/PSD Code. *Acta Phys. Polonica A* 5(141), 507-515.
- BERGER, M.J., HUBBELL, J.H., 1987. XCOM: Photon Cross Sections Database, Web Version 1.2. National Institute of Standards and Technology Gaithersburg, MD 20899, USA (available at <http://physics.nist.gov/xcom>). Jackson, D.F., Hawkes, D.J., 1981. X-ray attenuation coefficients of elements and mixtures, *Physics Reports*, 70, 169–233.
- CANTOR, B., CHANG, I.T.H., KNIGHT, P., VINCENT, A.J.B., (2004). Microstructural development in equiatomic multicomponent alloys. *Mater. Sci. Engineer. A*, 213, 375–377.
- CHEN, Y., CHEN, D., WEAVER, J., GIGAX, J., WANG, Y., MARA, N.A., FENSIN, S., MALOY, S.A., MISRA, A., LI, N., (2023). Heavy ion irradiation effects on CrFeMnNi and AlCrFeMnNi high entropy alloys. *J. Nucl. Mater.*, 574, 154163.
- HAN, I. & DEMIR, L. (2009). Studies on effective atomic numbers, electron densities from mass attenuation coefficients in TixCo1-x and CoxCu1-x alloys. *Nucl. Instr. Methods B*, 267, 3505–3510.
- HAN, I. & DEMIR, L. (2010). Studies on effective atomic numbers, electron densities and mass attenuation coefficients in Au alloys. *J. X-ray Sci. Tech.*, 18, 39–46.
- HARIMA, Y., SAKAMOTO, Y., TANAKA, S., KAWAI, M., (1986). Validity of geometric progression formula in approximating gamma-ray buildup factors. *Nucl. Sci. Engineer.* 94, 24–35.
- HARIMA, Y., (1993). An historical review and current status of buildup factor calculations and applications. *Radiat. Phys. Chem.* 41, 631–672. ANSI/ANS 6.4.3. Gamma-ray Attenuation Coefficients and Buildup Factors for Engineering Materials. American

- Nuclear Society, La Grange Park, Illinois, (1991).
- JIANG, H., ZHANG, H., HUANG, T., LU, Y., WANG, T., LI, T., (2016). Microstructures and mechanical properties of Co₂MoxNi₂VW_x eutectic high entropy alloys. *Mater. Design*, 109, 539–546.
- JIANG, H., HAN, K., QIAO, D., LU, Y., CAO, Z., LI, T., (2018). Effects of Ta addition on the microstructures and mechanical properties of CoCrFeNi high entropy alloy. *Mater. Chem. Phys.*, 210, 43-48.
- JIAO, W., MIAO, J., LU, Y., CHEN, X., REN, Z., YIN, G., LI, T., (2023). Designing CoCrFeNi-M (M = Nb, Ta, Zr, and Hf) eutectic high-entropy alloys via a modified simple mixture method. *J. Alloys Comp.*, 941, 168975.
- JIE, Z.J., CAO, J.C., RUAN, Z.Q., LI, H.H., (2014). A promising new class of high-temperature alloys: eutectic high-entropy alloys. *Sci. Rep.*, 4, 6200.
- LI, S., CHEN, F., TANG, X., GE, G., SUN, Z., GENG, Z., FAN, M., & HUANG, P., (2022). Effect of Ti on the Microstructure and Mechanical Properties of AlCrFeNiTi_x Eutectic High-Entropy Alloys. *J. Mater. Engineer. Perform.*, 31, 8294–8303.
- LU, Y.P., DONG, Y., GUO, S., JIANG, L., KANG, H.J., WANG, T.M., WEN, B., WANG, CHEN, X., XIE, W., ZHU, J., WANG, Z., WANG, Y., MA, Y., YANG, M., JIANG, W., YU, H., WU, Y., & HUI, Y., (2021). Influences of Ti Additions on the Microstructure and Tensile Properties of AlCoCrFeNi_{2.1} Eutectic High Entropy Alloy. *Intermetallics*, 128, 107024.
- MANOHARA, S.R., HANAGODIMATH, S.M. (2007). Studies on effective atomic numbers and electron densities of essential amino acids in the energy range in energy range 1 keV-100 GeV. *Nucl Instrum. Methods B* 258, 321-328.
- MUKARRAM, M., MUJAHID, M., YAQOUB, K., (2021). Design and development of CoCrFeNiTa eutectic high entropy alloys. *J. Mater. Res. Tech.*, 10, 1243-1249.
- SAKAR, E., (2020). Determination of photon-shielding features and build-up factors of nickel–silver alloys. *Radiat. Phys. Chem.* 172, 1-13.
- SAKAR, E., OZPOLAT, O.F., ALIM, B., SAYYED, M.I., KURUDIREK, M., 2020. Phy-X / PSD: Development of a user friendly online software for calculation of parameters relevant to radiation shielding and dosimetry. *Radiat. Phys. Chem.* 166, 108496.
- SAKAR, E. GULER, O., ALIM, B., SAY, Y., DIKICI, B., (2023). A comprehensive study on structural properties, photon and particle attenuation competence of CoNiFeCr-Ti/Al high entropy alloys (HEAs). *J. Alloys Comp.*, 931, 167561.
- SAYYED, M., MOHAMMED, F.Q., MAHMOUD, K.; LACOMME, E., KAKY, K.M., KHANDAKER, M.U., FARUQUE, M.R.I. (2020). Evaluation of Radiation Shielding Features of Co and Ni-Based Superalloys Using MCNP-5 Code: Potential Use in Nuclear Safety. *Appl. Sci.* 10, 7680.
- WANG, Y., LI, S., CHEN, F., YANG, K., GE, G., TANG, X., FAN, M., HUANG, P., (2023). Unique dislocation loops distribution of AlCrFeNiTi_x eutectic high-entropy alloys under high-temperature ion irradiation, *J. Alloys Comp.*, 170373.
- WOOD, J. Computational methods in reactor shielding, Elsevier (2013).
- XIANG, C., HAN, E.H., ZHANG, Z.M., FU, H.M., WANG, J.Q., ZHANG, H.F., et al., (2019). Design of single-phase high-entropy alloys composed of low thermal neutron absorption cross-section elements for nuclear power plant application. *Intermetallic* 104, 143-53.
- XIAO, J.-K., TAN, H., CHEN, J., MARTINI, A., ZHANG C., (2020). Effect of carbon content on microstructure, hardness and wear resistance of CoCrFeMnNiC_x high-entropy alloys. *J. Alloy. Compd.*, 847, 156533.
- YEH, B.J.W., CHEN, S.K., LIN, S.J., GAN, J.Y., CHIN, T.S., SHUN, T.T., TSAU, C.H., CHANG, S.Y., (2004). Nanostructured high-entropy alloys with multiple principal elements: novel alloy design concepts and outcomes *Advan. Engineer. Mater.*, 6(5), 299-303.